Heliyon 10 (2024) e29797

Contents lists available at ScienceDirect

Heliyon

journal homepage: www.cell.com/heliyon

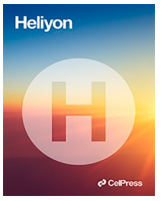

Research article

Pure total flavonoids from Citrus ameliorate NSAIDs-induced intestinal mucosal injury via regulation of exosomal LncRNA H19 and protective autophagy

Shanshan Chen [a,1], Ruonan He [b,1], Ying Li [c], Shuo Zhang [d,*]

[a] *The First Affiliated Hospital of Zhejiang Chinese Medical University (Zhejiang Provincial Hospital of Traditional Chinese Medicine), Hangzhou, 310053, Zhejiang, China*
[b] *The First Clinical Medical College, Zhejiang Chinese Medical University, Hangzhou, 310053, Zhejiang, China*
[c] *The Second Affiliated Hospital of Zhejiang Chinese Medical University (The Xin Hua Hospital of Zhejiang Province), Hangzhou, 310053, Zhejiang, China*
[d] *The Second Affiliated Hospital of Zhejiang Chinese Medical University (The Xin Hua Hospital of Zhejiang Province), No. 318 Chaowang Road, Hangzhou, 310005, Zhejiang, China*

A R T I C L E I N F O

Keywords:
PTFC
NSAIDs
Intestinal lesions
Exosomal lncRNA H19
Autophagy
Intestinal mucosal mechanical barrier

A B S T R A C T

Introduction: Non-steroid anti-inflammatory drugs (NSAIDs) are a class of prescription drugs with antipyretic, analgesic, anti-inflammatory, and antiplatelet effects. However, long-term use of NSAIDs will disrupt the intestinal mucosal barrier, causing erosion, ulcers, bleeding, and even perforation. Pure total flavonoids from Citrus (PTFC) is extracted from the dried peel of Citrus, showing a protective effect on intestinal mucosal barrier with unclear mechanisms.

Methods: In the present study, we used diclofenac (7.5 mg kg^{-1}, i.g.) to induce a rat model of NSAIDs-related intestinal lesions. PTFC (50, 75, 100 mg·kg−1 d−1, i.g.) was administered 9 days before the initial diclofenac administration, followed by co-administration on the last 5 days. Exosomes were identified by western blotting and transmission electron microscopy (TEM), and then co-cultured with IEC-6 cells. The expression of long non-coding RNA (lncRNA) H19, autophagy-related 5 (Atg5), ZO-1, Occludin, and Claudin-1 were detected by quantitative real-time PCR (qRT-PCR). The expression of light chain 3 (LC3)-I, LC3-II, ZO-1, Occludin and Claudin-1 proteins was tested by western blotting. The localization of both exosomes and autophagosomes was examined by immunofluorescent technique.

Results: The treatment of PTFC attenuated intestinal mucosal mechanical barrier function disturbance in diclofenac-induced NSAIDs rats. IEC-6 cells co-cultured with NSAIDs rats-derived exosomes possessed the lowest levels of protective autophagy, and severe intestinal barrier injuries. Cells co-cultured with the exosomes extracted from rats administrated PTFC exhibited an improvement of autophagy and intestinal mucosal mechanical barrier function. The prevention effect was proportional to the concentration of PTFC administered.

Conclusion: PTFC ameliorated NSAIDs-induced intestinal mucosal injury by down-regulating exosomal lncRNA H19 and promoting autophagy.

* Corresponding author.
E-mail addresses: chenshanshan198848@126.com (S. Chen), hrn1223@163.com (R. He), liying0821y@163.com (Y. Li), zhangshuotcm@126.com (S. Zhang).
[1] These authors contributed equally to this work.

https://doi.org/10.1016/j.heliyon.2024.e29797
Received 23 November 2023; Received in revised form 8 April 2024; Accepted 15 April 2024
Available online 26 April 2024

1. Introduction

Non-steroid anti-inflammatory drugs (NSAIDs), a category of drugs that do not contain steroid structures, are widely used in clinics because of their excellent antipyretic, anti-inflammatory, and analgesic effects [1]. Today, NSAIDs have become one of the most widely used prescription drugs worldwide, used by approximately 30 million persons daily [2]. With the increasing use of NSAIDs, the clinical safety of the drugs has gradually attracted the attention of clinicians, patients, and society [3]. U.S. Food and Drug Administration (FDA) announces that NSAIDs have a potential risk of gastrointestinal bleeding, especially in the lower gastrointestinal (GI) tract [4]. Long-term use of NSAIDs will cause erosions, ulcers, strictures, bleeding, and perforation of the intestinal mucosa, seriously endangering health [5]. Presently, proton pump inhibitors (PPIs), mucosal protective agents, and symptomatic treatment are mainly used to treat the GI injury caused by NSAIDs, but the effects are not apparent [6]. The crucial measure is to clarify the pathogenesis and aggravation mechanism of NSAIDs-related intestinal lesions, thus finding suitable symptomatic drugs to prevent the clinical side effects of NSAIDs.

The intestinal mucosal mechanical barrier dysfunction may be the core mechanism of intestinal lesions caused by NSAIDs [7]. The physiological structure of the intestinal mucosal mechanical barrier is based on intestinal epithelial cells (IECs) and tight junctions, whose structural integrity and functional well-being take an essential role in maintaining intestinal homeostasis [8]. NSAIDs-induced impairment of intestinal mucosal mechanical barrier structure and function will increase intestinal mucosa permeability, leading to mucosal lesions such as ulcers, bleeding, and perforation. Protecting the function of the intestinal mechanical barrier may be crucial in the prevention and treatment of the NSAIDs induced intestinal lesions.

Improving cellular protective autophagy may be essential to protecting intestinal barrier function. Some studies have found that autophagy is directly involved in regulating intestinal epithelial tight junctions, closely related to the intestinal mucosal mechanical barrier [9]. Our previous research confirmed the relationship between the intestinal mucosal mechanical barrier and autophagy. Increasing the level of autophagy via phosphoinositide 3-kinase/protein kinase B/mechanistic target of rapamycin kinase (PI3K/Akt/mTOR) pathway will improve the intestinal mucosal mechanical barrier function, treating intestinal mucosal damage of NSAIDs rats [10]. Regulation of cellular autophagy to maintain normal intestinal mucosal mechanical barrier function may be a feasible mechanism to lighten NSAID-induced intestinal lesions.

lncRNA H19, a newly discovered lncRNA, is directly related to autophagy and intestinal mucosal mechanical barrier dysfunction. lncRNA H19 could promote the phosphorylation of mTOR by inhibiting DIRAS Family GTPase 3 (DIRAS3) expression and thus inhibiting cellular autophagy [11]. lncRNA H19 could also affect autophagy by regulating PI3K/AKT/mTOR pathway [12]. lncRNA H19 has been directly proved to be a critical regulator gene in IECs, which causes intestinal mucosal mechanical barrier dysfunction by inhibiting the autophagy of IECs [13]. lncRNA H19, which could regulate autophagy and subsequent intestinal mucosal mechanical barrier function, is expected to be an essential target for preventing NSAIDs-related intestinal lesions.

Exosomes are one type of nano-sized extracellular vehicles (EVs) secreted by cells, containing abundant RNA, including long noncoding RNA (lncRNA), messenger RNA (mRNA), and microRNA (miRNA), which will be transported and mediate the transfer of substances, and information between cells, thereby affecting the signaling pathways in target cells and achieving cellular cascade reaction [14,15]. Once exosomes are phagocytosed by cells, the inside RNA will activate intracellular signaling pathways, resulting in corresponding physiological functions [16].

Increasing studies have linked exosomes with lncRNA H19, revealing the importance of exosomal lncRNA H19. lncRNA H19 in exosomes secreted by bile duct epithelial cells will promote the activation of adjacent normal hepatic stellate cells (HSCs), resulting in the exacerbation of cholestatic hepatic fibrosis [17,18]. $CD90^{+}$ hepatocellular carcinoma (HCC) cells modulate endothelial cell phenotype by releasing exosomes containing lncRNA H19 [19]. Chen, Yang et al. have found that exosomes containing lncRNA H19 secreted by mesenchymal stem cells (MSCs) will induce the invasion and migration of trophoblast cells [20]. Ren, Jing et al. found that carcinoma-associated fibroblasts promote colorectal cancer (CRC) stemness and chemoresistance by transcellular transfer of exosomal lncRNA H19 [21]. lncRNA H19 may enter normal cells with the help of exosomes and activate disease-related pathways, causing lesions of normal cells. Therefore, it is necessary to clarify whether exosomes are an intermediate tool for lncRNA H19 to inhibit autophagy and intestinal mucosal mechanical barrier function in normal IEC cells, resulting in the deterioration of NSAIDs-related enteropathy.

Pure total flavonoids from Citrus (PTFC) is a natural flavonoid polymer isolated and purified from the dried peel of *Citrus changshan-huyou* [Hybrid of orange of *Citrus grandis (L.) Osbeck* and *Citrus sinensis (L.) Osbeck*], mainly composed of naringin, neohesperidin, and narirutin [22]. The previous study of the research group has confirmed that the treatment of PTFC could promote cellular autophagy levels and improve the intestinal mucosal mechanical barrier dysfunction caused by NSAIDs, achieving the purpose of treating NSAIDs-related mucosal lesions [10]. *Citrus changshan-huyou*, also known as "Qu Zhi Qiao", is mainly produced in Changshan, Zhejiang Province. *Citrus changshan-huyou* is a new source of traditional Chinese medicinal material "Fructus Aurantii Immaturus". In addition, as authentic medicinal material, it was selected as the new "Zhejiang Eight Flavours". *Citrus changshan-huyou* has an excellent anti-inflammatory effect, therefore, it is also commonly used in the clinical treatment of inflammatory bowel disease and enteropathy caused by NSAIDs [23]. However, because of the strict processing requirements of *Citrus changshan-huyou*, its extract PTFC may have a better prospect for clinical promotion.

Combined with the previous research of the research group and literature analysis, we believe that the regulation of autophagy and intestinal mucosal mechanical barrier does exist. However, the correlation between lncRNA H19, autophagy/the intestinal barrier, and exosome remains unclear. Therefore, in the study, we aimed to explore 1) whether PTFC could prevent the side effects of NSAIDs-intestinal mucosal injury, 2) whether exosomal lncRNA H19 could transcellular regulate autophagy and intestinal mucosal

mechanical barrier, 3) whether exosomal lncRNA H19 is a critical target of PTFC.

2. Materials and methods

2.1. Rats care

Thirty SD rats (eight-week-old, 220 ± 20 g, male), specific pathogen-free (SPF) grade, were purchased from Shanghai SLAC Laboratory Animal Co., Ltd (SCXK(Hu) 2021-0005). Rats were housed in an environment with a temperature of 20 ± 2 °C, relative humidity of 60 ± 5 %, a light/dark cycle of 12h each, and allowed food and water ad libitum. The animal study was approved by the Institutional Animal Care and Use Committee of Zhejiang Chinese medical university (Approval No. IACUC-20210712-10). All animal care (including the euthanasia procedure) was done with the guidelines of the Association for Assessment and Accreditation of Laboratory Animal Care (AAALAC) and the Institutional Animal Care and Use Committee (IACUC).

2.2. Drug administration and rat modeling

After one week of acclimation, male SD rats were randomly divided into the Control, NSAIDs, PTFC (low), PTFC (medium), and PTFC (high) groups (six SD rats in each group). In the NSAIDs group, SD rats were administered diclofenac (7.5 mg kg^{-1}, i.g.) twice a day for five days to induce intestinal lesions [24]. In the PTFC groups, SD rats were administered PTFC (50, 75, 100 mg kg^{-1} d^{-1}, i.g.) for nine days, and then both PTFC and diclofenac (7.5 mg kg^{-1}, i.g. twice a day) were co-administered for the next five days. SD rats in the control group were administered the same dose of saline solution (Sodium chloride 0.9 % in aqueous solution, i.g.). The SD rats were anesthetized and sacrificed after fasting for 24 h (9 a.m.–9 a.m. the next day), and small intestines were collected for the subsequent experiments. The diclofenac modeling result and the preventive effect of PTFC in the study were judged by observing the small intestinal mucosa of SD rats.

2.3. Analysis of PTFC component

PTFC is extracted from the dried peel of *Citrus changshan-huyou* Y. B chang [Hybrid of orange of *Citrus grandis (L.) Osbeck* and *Citrus sinensis (L.) Osbeck*]. The extraction method of PTFC has obtained the invention patent of China (ZL201110269192.2). The main components of PTFC were determined by High-Performance Liquid Chromatography (HPLC) analysis.

2.4. Exosomes extraction

The method of small intestinal exosome extraction was referred the Master dissertation [25]. The exosome extraction process is as follows: 1) Small intestinal tissue was cut as segments of 4–6 cm, and its small intestinal epithelium was entirely exposed. 2) After rinsing with phosphate-buffered saline (PBS) three times, 10 mM dithiothreitol (DTT) was used to remove the mucus. 3) The tissues were soaked in 8 mM ethylenediaminetetraacetic acid (EDTA) for 30 min. 4) After the centrifugation at 300*g* for 5 min, the pellet was discarded. 5) An equal volume of ExoQuick® exosome solution (System Biosciences, USA) was added and stored at 4 °C overnight. 6) Centrifuging at 1500 g for 30 min, the precipitate is seen as the enriched intestinal exosomes. 7) A part of the exosomes was used for identification, and the remaining were resuspended in TRIzol™ LS (Thermo Fisher Scientific, USA) and stored at −80 °C for later analysis.

2.5. Identification of exosomes

2.5.1. Identification via transmission electron microscope (TEM)

The TEM identification process is as follows: 1) 5 μl of exosome solution (resuspended in PBS) was placed on the copper mesh with a

Table 1
Information of antibodies.

Antibody	Company/Cat	Dilution	Molecular weight (kDa)
Primary antibody			
CD63	Santa Cruz/SC-365604	1:300	50
TSG101	Santa Cruz/SC-7964	1: 500	45
CD9	Santa Cruz/SC-13118	1: 500	9
β-actin	Abcam/ab8226	1: 5000	42
ZO-1	Santa Cruz/SC-33725	1: 400	220
Claudin-1	Abcam/ab15098	1: 500	19
Occludin	Abcam/ab167161	1: 50000	59
LC3A/B	CST/4108	1: 1000	14/16
GAPDH	Abcam/ab181602	1:10000	36
Secondary antibody			
Goat anti-Mouse IgG (H + L) (HRP)	Thermo Pierce 31431	1: 5000	/
Goat anti-Rabbit IgG (H + L) (HRP)	Thermo Pierce 31210	1: 5000	/

diameter of 2 mm. 2) 2 % phosphotungstic acid solution was used to perform negative stain at room temperature (rt) for 10 min. 3) After blotting the negative staining solution with filter paper, the copper mesh was baked under an incandescent lamp for 2 min. 4) The copper mesh was placed under a Tecnai™ G2 Spirit TEM (FEI Company, USA) at 80 kV to observe the exosome morphology.

2.5.2. Identification via western blotting (WB)

The WB identification process is as follows: 1) The extracted exosomes were added to an equal volume of exosome-specific lysis buffer (Umibio, cat: UR33101), lysed on ice, and centrifuged (4 °C) at 12,000 g for 10min to take the supernatant liquid. 2) BCA (bicinchoninic acid) assay protein quantification kit (MULTI SCIENCES, cat: PQ0012) was used for determining protein concentration. Diluting protein concentration to 1 μg/μl 3) Proteins (10 μg) were loaded on 10 % sodium dodecyl sulfate-polyacrylamide gel electrophoresis (SDS–PAGE) gels (BIO-RAD, cat:#1610183) for electrophoresis and transferred to polyvinylidene difluoride (PVDF) membranes (Millipore, cat: IPVH00010) by the Trans-Blot Turbo system (BIO-RAD, USA) semidry transfer (1.3A, 25V, 5min). 4) Three exosome marker proteins, CD9, CD63, and TSG101, were selected as detection indicators. The PVDF membranes were incubated overnight with the corresponding primary antibodies (CD9, CD63, TSG101, and β-Actin) at 4 °C, followed by incubation with the secondary antibodies. All information on the used antibodies can be found in Table 1. Thermo Scientific SuperSignal West Dura kit (Thermo Fisher Scientific, cat: 34075) was used to prepare enhanced chemiluminescence (ECL) solution. X-ray film (HUADONG MEDICINE, China) was used to visualize the protein band in a dark room. β-actin was seen as the standard reference.

2.6. Exosomal lncRNA H19 detection

The TRIzol® Plus RNA Purification Kit (Thermo Fisher Scientific, cat: 12183-555) was used to extract RNA from exosomes, and the RNase-Free DNase Set (Qiagen, cat: 79254) was used to clear residual DNA. BioDrop μLITE+ (BioDrop, UK) was used to determine the concentration and quality of extracted RNA, and then RNA concentration was uniformly diluted to 125 ng/μl. Real-Time Quantitative Reverse Transcription Polymerase Chain Reaction (qRT-PCR) is performed, and the process is as follows: 1) According to the manufacturer of SuperScript™ III First-Strand Synthesis SuperMix for qRT-PCR (Thermo Fisher Scientific, cat: 11752-050), the reverse reaction condition was performed with 10 min at 25 °C, 30 min at 50 °C and 5 s at 85 °C. 2) 10 μl qRT-PCR amplification system includes 2 μl cDNA, 5 μl 2xSuper SYBR green, 0.4 μl forward prime of lncRNA H19 (10 μm), 0.4 μl reverse primer of lncRNA H19 (10 μm), and 2.2 μl ddH2O. Primer sequences were designed by Primer Premier 6.0 (Premier Biosoft, USA), Beacon designer 7.8(Premier Biosoft, USA), and synthesized by Sangon Biotech Co., Ltd (Table 2). The Power SYBR® Green PCR Master Mix (Applied Biosystems, cat: 4367659) and CFX384 Touch Real-Time PCR Detection System (BIO-RAD, USA) were used in the amplification reaction. The reaction condition was pre-denaturation at 95 °C for 1 min, denaturation at 95 °C for 10 s, annealing and extension at 60 °C for 25 s for 40 cycles. Three replicate wells were set for each sample. The relative expression of lncRNA H19 was calculated using the $2^{-\Delta\Delta}$Ct method [26].

2.7. Cell culture

IEC-6 cells, epithelial cells of rat small intestine [27], were purchased from American Type Culture Collection (ATCC, USA) and cultured in Dulbecco's Modified Eagle Medium (DMEM) (Gibco, cat: 11995-040) supplemented with 10 % fetal bovine serum (FBS) (Gibco, cat: 10099141) and 0.1 Unit/ml human insulin (Sigma, cat: I9278). The cells were cultured in a 37 °C incubator containing 5 % CO_2.

2.8. LncRNA H19 interference

LncRNA H19 interfering lentivirus and control lentivirus are provided by Genechem (Shanghai). The specific information is as follows. lncRNA H19: NR_027324.1; vector information: pLKO.1 interference vector. After transfection, puromycin (2.0 μg/ml) was used to select the lncRNA H19 shRNA-stabilized IEC-6 cells for the subsequent experiments. The efficiency of silencing was confirmed

Table 2
mRNA primer sequences.

Gene	Genbank Accession	Primer Sequences (5′to3′)	Size (bp)
lncRNA H19	NR_027324.1	F:CAGGAATCGGCTCGAAGGTAAAG R: GTGCTGTGTGGGTCTGCTCTT	74
Atg5	NM_001014250.1	F: TCAGCTCTGCCTTGGAACATCA R: AAGTGAGCCTCAACTGCATCCTT	95
ZO-1	NM_001106266.1	F: GACCCTGACCCAGTGTCTGATAA R: CTATCCCTTGCCCAGCTCTTCT	119
Occludin	NM_031329	F: CCAACGGCAAAGTGAATGGCAAGA R: CCACGGACAAGGTCAGAGGAATCT	105
Claudin-1	NM_031699.2	F: GTATGAATTTGGCCAGGCTCTCT R: GGACAGGAGCAGGAAAGTAG	87
GAPDH	NM_017008.4	F: GAAGGTCGGTGTGAACGGATTTG R: CATGTAGACCATGTAGTTGAGGTCA	127

by qRT-PCR.

2.9. IEC-6 and exosomes co-culture

The concentrations of exosomes extracted from the rats in the control, NSAIDs, and PTFC (low, medium, high) prevention groups were measured. The exosome concentration gradient of 50, 100, and 200 μg/ml was set. Referring to results of the experiment and literature [28,29]. We finally selected 200 μg/ml as the suitable exosome concentration for co-culture.

IEC-6 cells were cultured in Petri dishes for 12 h. The cells were then divided into 15 groups: IEC-6+Ctrol Exo, IEC-6+NSAIDs Exo, IEC-6+$PTFC_{low}$ Exo, IEC-6+$PTFC_{medium}$ Exo, IEC-6+$PTFC_{high}$ Exo, Scramble + Ctrol Exo, Scramble + NSAIDs Exo, Scramble + $PTFC_{low}$ Exo, Scramble + $PTFC_{medium}$ Exo, Scramble + $PTFC_{high}$ Exo, shRNA-H19+Ctrol Exo, shRNA-H19+NSAIDs Exo, shRNA-H19+$PTFC_{low}$ Exo, shRNA-H19+$PTFC_{medium}$ Exo, shRNA-H19+$PTFC_{high}$ Exo. Culture in DMEM supplemented with Exosome-depleted FBS (SBI, cat: EXO-FBS-50A-1). After co-cultivation for 48 h, cells in each group were collected for immunofluorescence, qRT-PCR, WB, and other subsequent assays.

2.10. Exosome endocytosis assay

The exosomes were labeled with PKH26 probe (red fluorescence), the lipophilic dye stably binding to the lipid bilayer membrane of exosomes, to determine whether the co-cultured exosomes could be swallowed by IEC-6 cells. The operational process is as follows. 1) The rat small intestine-derived exosomes were stained with PKH26 Red Fluorescent Cell Linker Kits (Sigma, cat: MIDI26) at rt for 5 min. 2) Adding an equal volume of Exosome-depleted FBS to stop staining and bind excess dye (rt, 1min). 3) Stained exosomes were co-cultured with IEC-6 cells for 12 h. 4) 4′6-diamidino-2-phenylindole (DAPI) was used to stain the cellular nucleus. The fluorescence microscope (Olympus, JPN) was selected for observing and picturing (200 ×).

2.11. Cellular autophagy detection

2.11.1. Determination of mRNA expression of autophagy-related genes

Total RNA was extracted from IEC-6 cells for qRT-PCR to detect the expression of autophagy-related gene Atg5 mRNA (Table 2). The experimental process is consistent with the previous qRT-PCR analysis of exosomal lncRNA H19.

2.11.2. Determination of protein expression of autophagy-related genes

1) Whole Cell Lysis Assay (KeyGEN, cat: KGP2100) was used to extract protein from IEC-6 cells. 2) The protein concentration was detected by the BCA method protein quantification kit (MULTI SCIENCES, cat: PQ0012) and uniformly diluted to 5 μg/μl 3) Proteins (50 μg) were loaded on 12 % SDS–PAGE gels (BIO-RAD, cat:#1610185) for electrophoresis (180V, 40 min) and transferred to PVDF membranes (Millipore, cat: IPVH00010) by the semidry transfer for 1.3A, 25V, 4min. 4) The corresponding primary antibodies (LC3A/B) were added and incubated overnight at 4° on a shaker. The next day, the secondary antibodies were added and incubated for 1 h at rt (Table 1). 5) X-ray film (HUADONG MEDICINE, China) was used to visualize the protein band in a dark room. The band intensities were quantitated via Image Pro Plus 6.0 software (Media Cybernetics, USA) for three times. The average value was seen as the intensity of the band and used for further analysis. Data were presented as the ratios of target protein expression value to that of GAPDH.

2.11.3. Immunofluorescence (IF)

The experiment aimed to realize autophagosome localization and semi-quantitative analysis. 1) Cell slides (12-well plate) were prepared. 2) 4 % fresh paraformaldehyde was used to fix for 30 min, at 4 °C. 3) Using 0.5 % Triton X-100 (Beyotime, cat: P0096) treatment for 15 min to complete permeabilization. 4) Block with 10 % Normal Donkey Serum (Abcam, cat: ab7475) at rt for 30 min, then dilute the primary antibody with 1 % Normal Donkey Serum and incubate at 4 °C overnight. 5) Dilute the fluorescently labeled secondary antibody with 1 % Normal Donkey Serum, and incubate at rt for 1 h in the dark. 6) DAPI was used to stain the nucleus of IEC-6 cells. 7) Mount the slides with the ProLong™ Gold Antifade Mountants (cat: P10144), and then take pictures (× 630) with the confocal laser scanning microscope (Zeiss, GER). Information on the antibodies used is recorded in Table 3.

2.12. Intestinal mucosal mechanical barrier function detection

The experimental method is the same as above. The difference is that genes (ZO-1, Occludin, and Claudin-1) related to the intestinal barrier function were analyzed. Primer sequence information is listed in Supplementary Table S2.

Table 3
Information on antibodies used in immunofluorescence.

Antibody	Company	Cat	Dilution
LC3 A/B	CST	12741	1: 100
β-tubulin	CST	86298	1: 100
Donkey Anti-Mouse IgG H&L (Alexa Fluor® 647)	Abcam	ab150107	1: 400
Donkey Anti-Rabbit IgG H&L (Alexa Fluor® 488)	Abcam	ab150073	1: 400

Protein extraction and concentration determination experiments are the same as above. Proteins (50 μg) were loaded on 7.5 % SDS–PAGE gels (BIO-RAD, cat:#1610181) or 10 % SDS–PAGE gels (BIO-RAD, cat:#1610183) for electrophoresis (180V, 45–50 min) and transferred to PVDF membranes (Millipore, cat: IPVH00010) by the semidry transfer (1.3A, 25V, 5min for Claudin-1, Occludin, and GAPDH) or wet transfer (210 mA, 180min for ZO-1). PVDF membranes were incubated with the corresponding primary and secondary antibodies in turn and exposed for intensity analysis (Supplementary Table S1).

2.13. Statistical analysis

SPSS Statistics 25 (IBM, USA) and GraphPad Prism 8 (Graphpad Software Inc, USA) were used for data analysis and visualization. Data are expressed as the mean ± SD (standard deviation). In multiple group comparison ($n > 2$), one-way Analysis of Variance (ANOVA) was used for statistical analysis. A post hoc test was carried out using LSD (least significant difference) analysis (assuming homogeneity of variances) and Tamhane T2 test (assuming heterogeneity of variance). All experiments were performed with three biological replicates. $P < 0.05$ was used to indicate statistical significance.

3. Results

3.1. Effects of diclofenac and PTFC on rats

Diclofenac-induced rat intestinal mucosal injury used in the study is a long-term modeling method for our research group with high feasibility and credibility (Fig. 1a) [10,24]. Additionally, because one of the crucial objectives of the study was to explore the preventive effect of PTFC on NSAIDs-related intestinal injury, we took a unique way of modeling. The rats in the PTFC intervention group were given different doses of PTFC for prevention in advance, and then diclofenac was given to induce intestinal mucosal lesions, simultaneously given PTFC for the prevention as well. The photos of rat small intestines further support the success of the modeling and the efficacy of PTFC in preventing intestinal mucosal injury. As shown in Fig. 1f, the small intestinal mucosa of rats in the NSAIDs group had apparent congestion and erosion compared with the normal group. In addition, the intestinal erosion of rats was improved in a PTFC dose-dependent manner (the higher the dosage, the better the improvement).

3.2. Compounds of PTFC

Previous analysis of our research group showed that the total flavonoid content (purity) of PTFC was 76.22 %. Among them, narirutin (Pubchem CID: 442431), naringin (Pubchem CID: 442428), hesperidin (Pubchem CID: 10621), and neo-hesperidin (Pubchem CID: 442439) were both the major flavonoids of PTFC, which contained 10.12 ± 0.12 μg/ml, 62.16 ± 2.67 μg/ml, 6.49 ± 0.10 μg/ml, and 49.28 ± 4.55 μg/ml, respectively [22]. Meanwhile, naringin/narirutin and hesperidin/neo-hesperidin are isomers of each other (same molecular formula but different structure) (Fig. 1b–e). Naringin, the most abundant flavonoid in PTFC, has been confirmed to have the excellent effect of improving intestinal mucosa [30,31]. Flavonoids have excellent intestinal barrier protection [32]. The

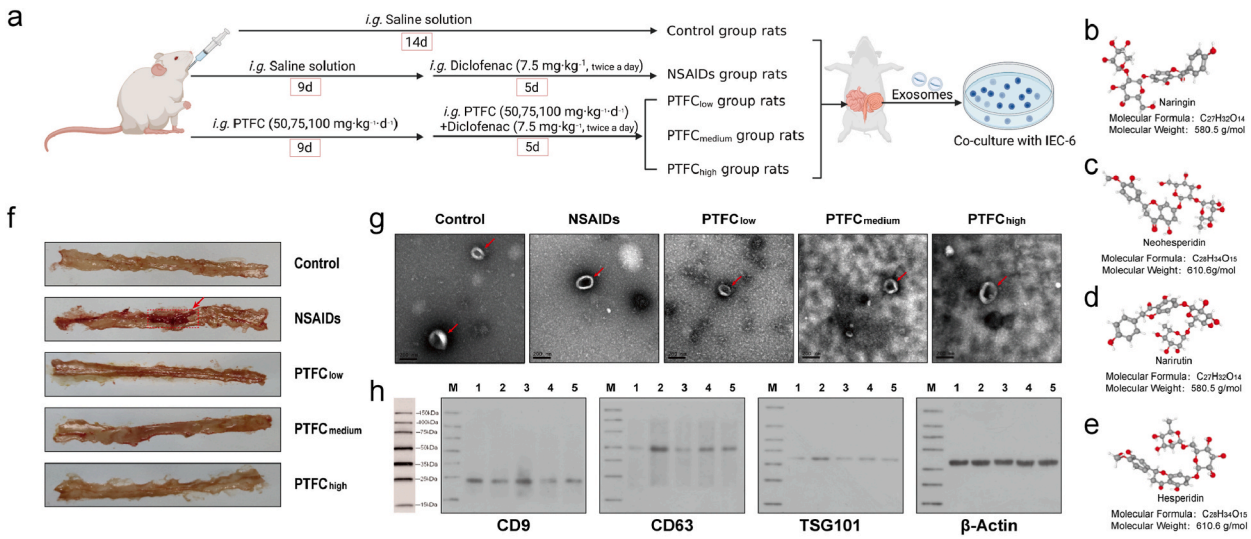

Fig. 1. NSAIDs-related intestinal lesion rat modeling, drug component analysis, and exosome extraction, identification. (a) Rat modeling and intestinal exosome extraction process. (b–e) Naringin, neo-hesperidin, narirutin, and hesperidin are the top four flavonoids with the highest concentration in PTFC. (f) Diclofenac will cause erosion of rat intestinal mucosa, while PTFC could treat diclofenac-induced intestinal lesions, and the improvement is proportional to the concentration of PTFC. (g–h) Exosomes were successfully extracted from the small intestines of rats. M: Marker, 1: Control, 2: NSAIDs, 3: PTFClow, 4: PTFCmedium, 5: PTFChigh.

study of Cao, Ruige et al. made it clear that naringin could treat dextran sulfate sodium (DSS)-induced intestinal mucosal injury in mice by improving intestinal barrier function [33]. Narirutin, hesperidin, and neo-hesperidin have the potential to improve intestinal mucosal barrier function because of their special effects on anti-inflammatory and oxidative stress [34–37].

3.3. Extraction and validation results of exosomes

Saucer-like shape exosomes are visible in the photos taken by TEM, supporting the success of rats intestinal tissue-derived exosome extraction (Fig. 1g). CD9 and CD63 are related to the secretion of exosomes, and TSG101 is involved in forming exosomes. So, the above proteins are all exosome marker proteins, which are helpful for the identification of exosomes [38,39]. Fig. 1h shows that CD9, CD63, and TSG101 were successfully detected in the extracted exosomes by the WB experiment, which also supports the success of the exosome extraction.

3.4. LncRNA H19 expression in rat intestines and exosomes

By detecting the expression of lncRNA H19 in rat intestines and exosomes, it is clear whether PTFC has a regulatory effect and whether expression changes of lncRNA H19 in exosomes converge with that in the rat small intestine. The expression of lncRNA H19 in diclofenac-induced NSAIDs rats' intestines and exosomes extracted from these rats' intestines was significantly higher than that of normal rats and exosomes. Meanwhile, the expression of lncRNA H19 in rat small intestinal tissue and exosomes decreased with the increase of PTFC concentration (Fig. 2a–b). The qRT-PCR results support a regulatory role of PTFC on the expression of rat intestinal and exosomal lncRNA H19.

3.5. Results of co-culture of exosomes with IEC-6 cells

3.5.1. Exosome endocytosis

Exosomes were labeled with PKH26 (red fluorescence) to determine whether the co-cultured exosomes would be phagocytosed by IEC-6 cells. The results showed apparent red fluorescence around the IEC6 cell nucleus (DAPI staining, showing blue fluorescence), indicating that the IEC6 cells, after co-culture, effectively phagocytosed the exosomes derived from the small intestine of rats (Fig. 3a–e).

3.5.2. lncRNA H19 expression

By detecting the expression of lncRNA H19 in IEC-6 cells co-cultured with exosomes derived from different rats, the effect of exosomes on the expression of lncRNA H19 in IEC-6 itself was clarified. The results showed that the expression of lncRNA H19 in IEC-6 co-cultured with NSAIDs rat-derived exosomes was significantly higher than in the normal group. Though the expression of lncRNA H19 in IEC-6 cells co-cultured with the exosomes extracted from the PTFC intervention group rats was higher than the normal group to a certain extent, there was still a decrease (lower than NSAIDs group). The improvement degree was positively correlated with the concentration of PTFC used in the intervention (Fig. 2c). The expression trend of lncRNA H19 in IEC-6 cells was consistent with the lncRNA H19 in exosomes used for co-culture. The result suggests that 1) exosomal lncRNA H19 will affect the IEC-6 cells' lncRNA H19, final resulting in a consistent trend 2) exosomes could indeed act as a tool for cell-to-cell information transfer.

3.5.3. Cellular autophagy

Microtubule Associated Protein 1 Light Chain 3 Alpha (MAP-LC3), also known as LC3, is involved in the whole process of autophagy. In the primary stage of autophagy, segmental polypeptides of cytoplasmic LC3 (i.e., LC3-I) will be enzymatically degraded. Then LC3-I will combine with phosphatidylethanolamine (PE), converting into membrane-type LC3 (i.e., LC3-II), gathering in

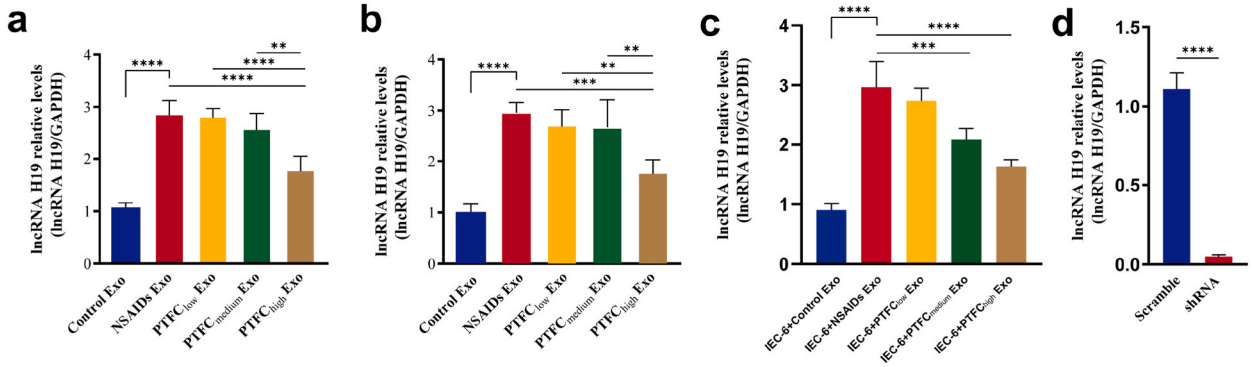

Fig. 2. lncRNA H19 expression results. (a) Rat intestines lncRNA H19 expression **(b)** Exosomal lncRNA H19 expression. **(c)** lncRNA H19 expression of the IEC-6 co-cultured with exosomes. **(d)** lncRNA H19 interference results. The data are presented as the mean ± SD, $^{**}p < 0.01$, $^{***}p < 0.001$, $^{****}p < 0.0001$.

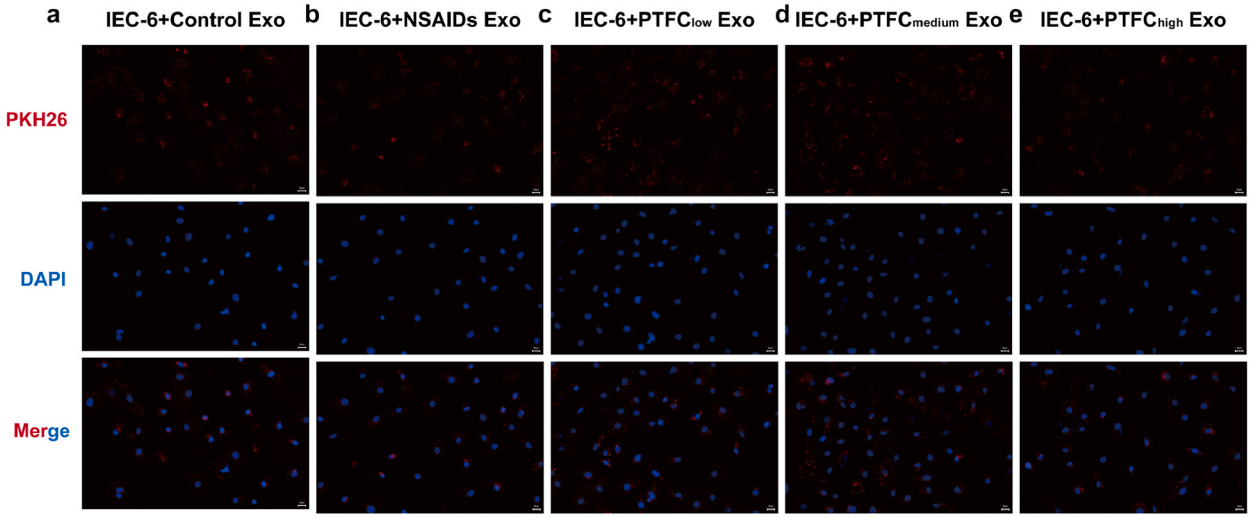

Fig. 3. Exosome endocytosis results. (a–e) IEC-6 cells could successfully engulf the exosomes extracted from rat small intestine.

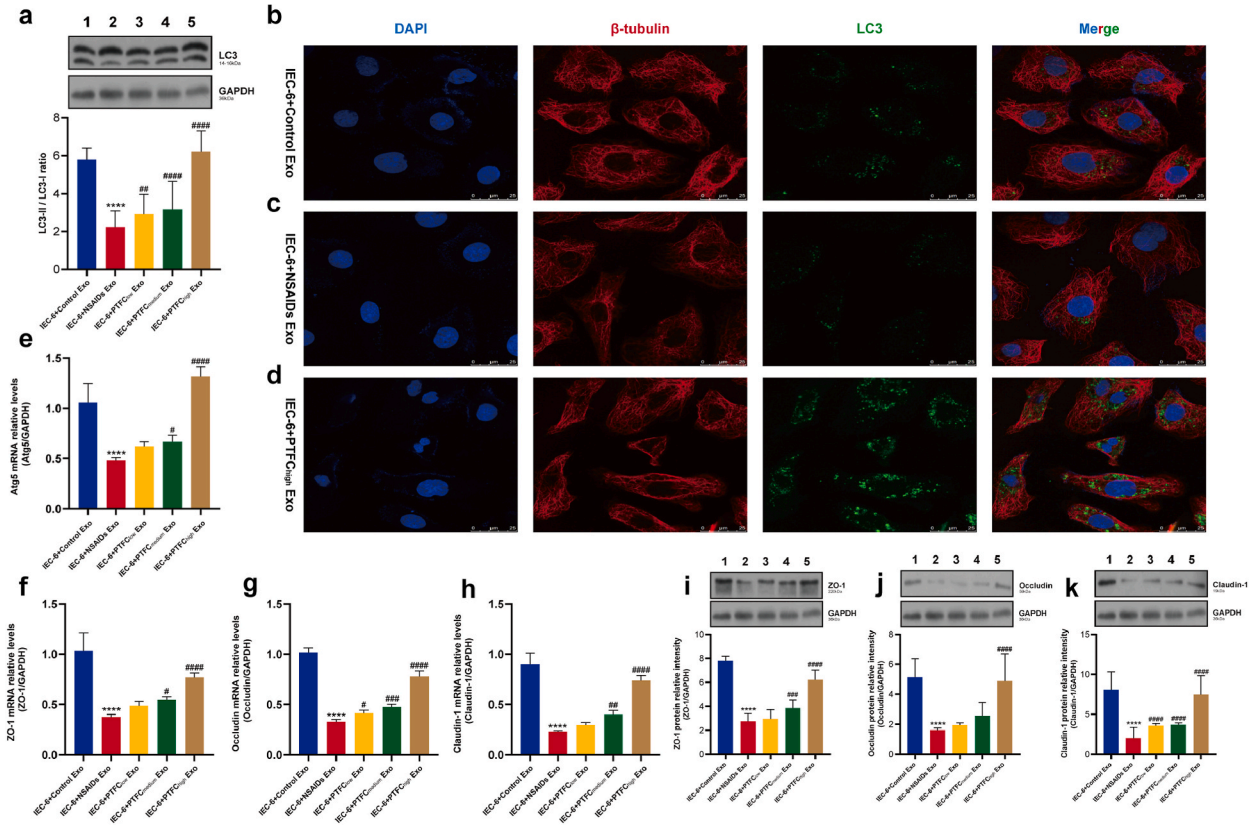

Fig. 4. Results of IEC-6 cells cultured with exosomes. (a) LC3-II/LC3-I protein expression ratio and the corresponding band. **(b-d)** LC3 is mainly expressed in the cytoplasm. After co-culture with exosomes from rats in the high-concentration PTFC prevention group, the LC3 fluorescence in IEC6 cells was enhanced, reflecting the increase in autophagosome generation. **(e)** Atg5 mRNA expression of the IEC-6 co-cultured with exosomes. **(f–h)** mRNA expression of intestinal mucosal mechanical barrier-related genes. **(i–k)** Protein expression of intestinal mucosal mechanical barrier-related genes. $^{****}p < 0.0001$ *vs.* IEC-6+Control Exo; $^{\#}p < 0.05$ *vs.* IEC-6+NSAIDs Exo, $^{\#\#}p < 0.01$ *vs.* IEC-6+NSAIDs Exo, $^{\#\#\#}p < 0.001$ *vs.* IEC-6+NSAIDs Exo, $^{\#\#\#\#}p < 0.0001$ *vs.* IEC-6+NSAIDs Exo.1: IEC-6+Control Exo, 2: IEC-6+NSAIDs Exo, 3: IEC-6+PTFC$_{low}$ Exo, 4: IEC-6+PTFC$_{medium}$ Exo, 5: IEC-6+PTFC$_{high}$ Exo.

autophagosomes [40]. Thus, LC3 was used as a marker protein of mammalian autophagy, while the ratio of LC3-II/I proteins was used to estimate autophagy levels. The WB results show that the ratio of LC3-II/I protein in IEC-6 cells co-cultured with NSAIDs rat-derived exosomes was significantly lower than that in IEC-6 cells co-cultured with normal rat-derived exosomes. The ratio of LC3-II/I protein of IEC-6 cultured with exosomes derived from rats in PTFC groups was increased, and the degree of improvement was proportional to the concentration of PTFC administered (Fig. 4a).

After co-culturing the exosomes from rats in the Control, NSAIDs, and $PTFC_{high}$ groups, IF was performed for localization and semi-quantitative analysis. Results showed that LC3 (green fluorescence) was primarily located in the cellular nucleus (DAPI staining, blue fluorescence) periphery and cytoskeleton (β-tubulin, staining with red fluorescence) internal, which suggests that LC3 was mainly expressed in the cytoplasm (Fig. 4b–d). In addition, after co-culture with exosomes derived from rats of high concentration PTFC treating group, the LC3 fluorescence in IEC6 cells was enhanced.

The occurrence of autophagy also depends on the participation of a series of autophagy-related (Atg) proteins, of which autophagy-related 5 (Atg5) is necessary for the formation of autophagosomes is relatively conservative and stable and exists in most eukaryotes. Atg5 promotes the formation of autophagosomes [41] and takes a vital role in the formation of the autophagic vacuole (AV) [42]. The results of qRT-PCR showed that Atg5 mRNA expression in IEC-6 cells co-cultured with NSAIDs rat-derived exosomes was dramatically decreased compared with IEC-6 cells co-cultured with normal rat-derived exosomes. But, the Atg5 mRNA expression of IEC-6 co-cultured with exosomes extracted from rats in the PTFC groups was increased, and the degree of improvement was proportional to the concentration of PTFC administered (Fig. 4e). The results show that NSAIDs rats-derived exosomes will inhibit the autophagy of IEC-6 cells. In contrast, exosomes extracted from rats in the PTFC prevention group could effectively reverse the tendency to decrease autophagy of IEC-6 cells.

3.5.4. *Intestinal mucosal mechanical barrier function*

Cell junctions refer to the particular connection structure formed in the contact area of the plasma membrane between adjacent cells, which is vital in strengthening Intestinal mucosal mechanical barrier function [43]. As a type of cell junctions, tight junctions, mainly composed of occludin, claudin, and ZO proteins, are particularly important in holding intestinal mucosal mechanical barrier function [44,45].

Therefore, we detected the expression of ZO-1, occludin, and claudin-1 to indirectly reflect the intestinal mucosal mechanical barrier function of IEC-6 cells. The results of qRT-PCR showed that ZO-1, occludin, and claudin-1 mRNA expression in IEC-6 cells co-cultured with NSAIDs rat-derived exosomes was much lower than in IEC-6 cells co-cultured with normal rat-derived exosomes. However, the ZO-1, occludin, and claudin-1 mRNA expression of IEC-6 cultured with exosomes derived from rats in the PTFC groups were increased with the addition of PTFC administrated concentration (Fig. 4f–h). The expression of ZO-1, occludin and claudin-1 protein in IEC-6 cells co-cultured with NSAIDs rat-derived exosomes was both significantly lower than that in IEC-6 cells co-

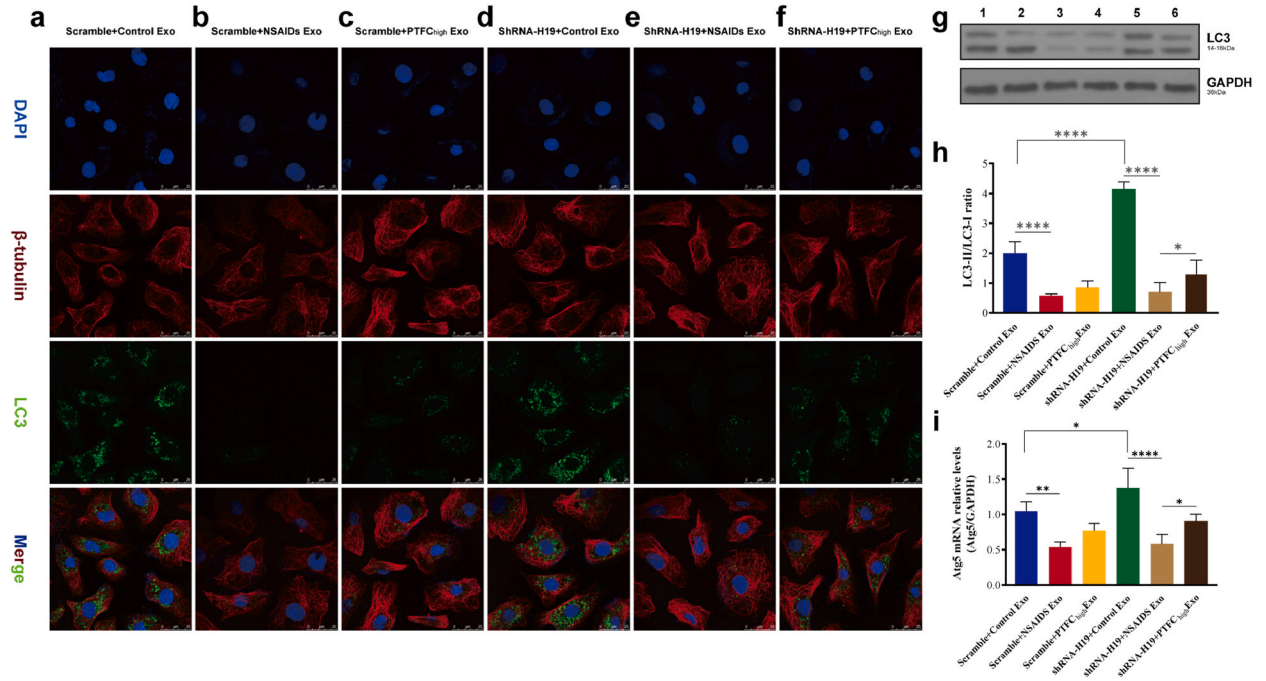

Fig. 5. Autophagy-related results of shRNA-H19 IEC-6 cells cultured with exosomes. (a–f) Autophagosome location and semi-quantitation results from shRNA-H19 IEC-6 co-cultured with control rats-derived exosomes. **(g)** LC3-II/LC3-I protein band, **(h)** LC3-II/LC3-I protein expression ratio. **i** Atg5 mRNA expression. $*p < 0.05$, $**p < 0.01$, $****p < 0.0001$. 1: scramble IEC-6+Control Exo, 2: 1: shRNA-H19 IEC-6+Control Exo, 3: scramble IEC-6+NSAIDs Exo, 4: shRNA-H19 IEC-6+NSAIDs Exo,5: scramble IEC-6+$PTFC_{high}$ Exo, 6: shRNA-H19 IEC-6+$PTFC_{high}$ Exo.

cultured with normal rat-derived exosomes. The expression of ZO-1, occludin, and claudin-1 protein of IEC-6 cultured with exosomes derived from rats in PTFC groups was increased, and the improvement was proportional to the concentration of PTFC administered (Fig. 4 i-k). The results show that exosomes derived from NSAIDs rats will disrupt the intestinal mechanical barrier function of IEC-6 cells. The exosomes derived from rats in the PTFC prevention group also damaged the function of the intestinal mucosal mechanical barrier of IEC-6 cells, but the degree was significantly lower than that in the NSAIDs group.

In the absence of additional intervention, co-culture with rat-derived exosomes alone resulted in changes in the autophagy level and intestinal mucosal mechanical barrier function of normal IEC-6 cells, and the changes were consistent with rat intestinal mucosal lesions. This result suggests that a particular substance in rat exosomes can affect the autophagy and intestinal barrier of IEC-6 cells, and this critical substance may be lncRNA H19, but still needs more verification.

3.6. Results of Co-culture of exosomes with lncRNA H19 interference IEC-6 cells

3.6.1. lncRNA H19 interference results

In order to clarify the regulatory relationship between lncRNA H19 and autophagy/intestinal mucosal mechanical barrier, we artificially suppressed the expression of lncRNA H19 in IEC-6 cells. Fig. 2d shows that compared with the IEC-6 cells in the Scramble control group, the expression of lncRNA H19 in the cells of the shRNA-H19 group was significantly reduced, indicating the success of the interference experiment.

3.6.2. Cellular autophagy

The differences between cells in the same groups (scramble or shRNA-H19 groups) were compared, respectively. The results showed the decreased LC3-II/I protein ratio of IEC-6 co-cultured with NSAIDs rat exosomes. In contrast, the LC3-II/I protein ratio of IEC-6 cells cultured with exosomes derived from rats in the $PTFC_{high}$ intervention group was higher than that of the former. However, the LC3-II/I protein ratio could not be restored to a level similar to the control (Fig. 5h). The differences of different IEC-6 cells (scramble/shRNA-H19) co-cultured with the same source of exosomes were then compared. It was found that the LC3-II/I protein ratio of IEC-6 cells in the shRNA-H19 group was significantly higher than that in the scramble group (Fig. 5g–h).

The IF results showed that LC3 was mainly expressed in the cytoplasm. After co-culture with exosomes derived from rats of the NSAIDs group, the LC3 fluorescence in IEC6 cells, both in the scramble or shRNA-H19 groups, was decreased. The fluorescent intensity of LC3 in the IEC-6 cells co-cultured with the exosomes extracted from the $PTFC_{high}$ prevention group rats was significantly higher than that in the NSAIDs group. In addition, the fluorescence intensity of LC3 in IEC-6 cells increased after knocking out lncRNA H19

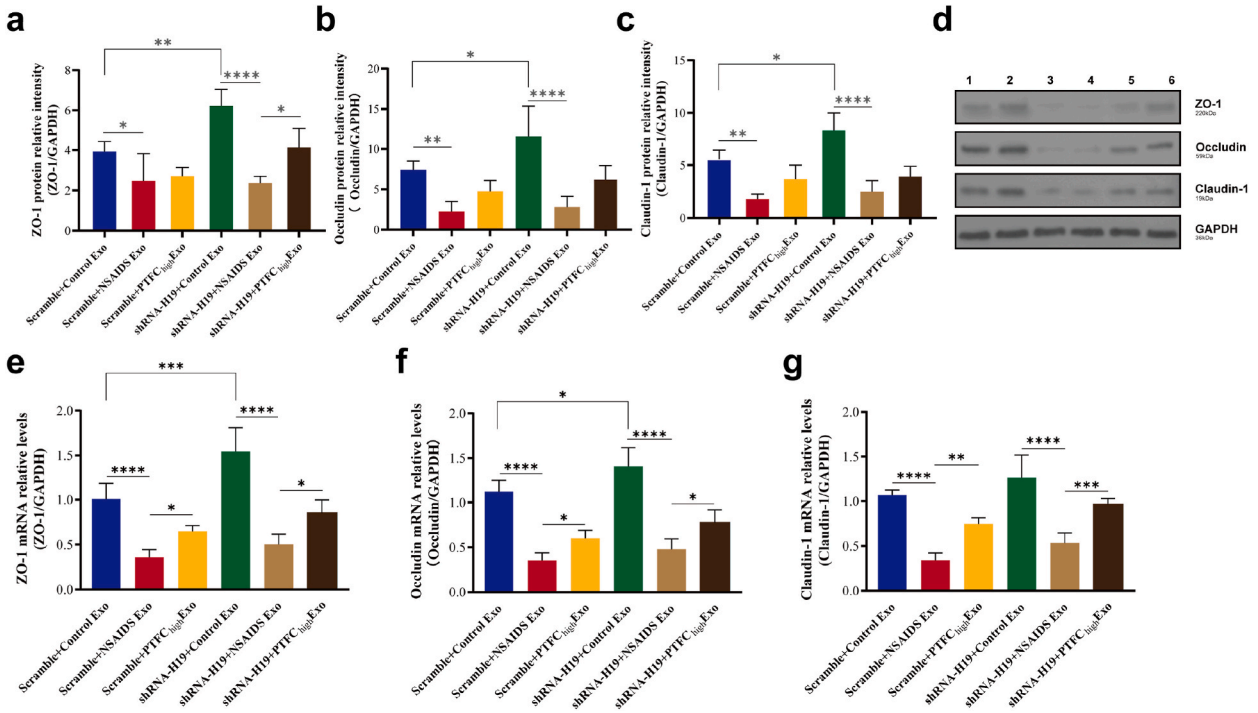

Fig. 6. Intestinal mucosal mechanical barrier-related results of shRNA-H19 IEC-6 cells cultured with exosomes. (a) ZO-1 protein expression, **(b)** occludin protein, **(c)** claudin-1 protein. **(d)** corresponding band, **(e)** ZO-1 mRNA expression, **(f)** Occludin mRNA, **(g)** Claudin-1 mRNA. *$p < 0.05$, **$p < 0.01$, ***$p < 0.001$, ****$p < 0.0001$. 1: scramble IEC-6+Control Exo, 2: 1: shRNA-H19 IEC-6+Control Exo, 3: scramble IEC-6+NSAIDs Exo, 4: shRNA-H19 IEC-6+NSAIDs Exo,5: scramble IEC-6+$PTFC_{high}$ Exo, 6: shRNA-H19 IEC-6+$PTFC_{high}$ Exo.

(Fig. 5a–f).

The results of qRT-PCR showed that compared with the IEC-6 cells (in the scramble or shRNA-H19 groups) co-cultured with control rat-derived exosomes, Atg5 mRNA expression in the IEC-6 cells co-cultured with the exosomes extracted from NSAIDs group rats was both dramatically decreased. The Atg5 mRNA expression of IEC-6 co-cultured with exosomes extracted from rats in the $PTFC_{high}$ prevention group was improved. Simultaneously, analysis of different IEC-6 cells (scramble/shRNA-H19) co-cultured with exosomes extracted from the same source showed that the interference of lncRNA H19 will increase Atg5 mRNA expression (Fig. 5i).

The above results suggested that 1) interference of IEC-6 lncRNA H19 did not significantly affect the tendency of autophagy of cells co-cultured with exosomes. Exosomes may primarily influence the cellular autophagy change trend, 2) inhibition of lncRNA H19 increase the autophagy levels in IEC-6 cells. lncRNA H19 may be a regulatory RNA of autophagy.

3.6.3. Intestinal mucosal mechanical barrier function

The results of WB showed that compared with the IEC-6 cells (in the scramble or shRNA-H19 groups) co-cultured with control rat-derived exosomes, intestinal mucosal mechanical barrier function-related protein (ZO-1, occludin, and claudin-1) expression in the IEC-6 cells co-cultured with the exosomes extracted from NSAIDs group rats was both dramatically decreased (Fig. 6a–c). Analysis of different IEC-6 cells (scramble/shRNA-H19) co-cultured with the same group of rats-derived exosomes showed that the interference of lncRNA H19 will increase the expression of ZO-1, occludin, and claudin-1 (Fig. 6a–d).

Fig. 6 e-g show that the expression of ZO-1, occludin, and claudin-1 mRNA in IEC-6 cells (in the scramble or shRNA-H19 groups) co-cultured with NSAIDs rat-derived exosomes was both significantly lower than that of IEC-6 cells co-cultured with normal rat-derived exosomes. The ZO-1, occludin, and claudin-1 mRNA expression of IEC-6 co-cultured with exosomes derived from rats in the $PTFC_{high}$ prevention groups were increased. Moreover, the expression of ZO-1, occludin, and claudin-1 mRNA will be increased after the interference of lncRNA H19.

The above results suggested that 1) Exosomes may be crucial in the regulating of intestinal mucosal mechanical barrier function, and 2) inhibition of lncRNA H19 improves the dysfunction of intestinal mucosal mechanical barrier in IEC-6 cells.

4. Discussion

The clinical mechanism of NSAIDs is: Inhibiting the synthesis of prostaglandin (PG), thereby exerting its anti-inflammatory, analgesic, and antipyretic effects. Due to the excellent clinical effects and low cost, NSAIDs have been widely used in clinics once their research and development (R&D).

Currently, NSAIDs have become one of the most widely used drugs worldwide. However, long-term use of NSAIDs will also cause a series of side effects. Among them, enteropathy caused by NSAIDs is extremely common. More than 60 % of patients taking long-term NSAIDs may have intestinal mucosal lesions [46]. Intestinal injury caused by NSAIDs includes increased intestinal mucosal permeability, erosion, ulcer, and may also have more serious clinical outcomes, such as perforation, obstruction, and death. Therefore, clarifying the mechanism of intestinal injury caused by NSAIDs and realizing prevention according to the disease mechanism in time may be effective in reducing the intestinal side effects of NSAIDs and improving the safety of clinical NSAIDs use.

In this study, we pre-administered PTFC before using diclofenac to induce intestinal injury in rats to explore the preventive effect of PTFC on NSAIDs enteropathy. PTFC is extracted from the dried peel of *Citrus changshan-huyou* [Hybrid of orange of Citrus grandis (L.) Osbeck and Citrus sinensis (L.) Osbeck], mainly composed of narirutin, naringin, hesperidin, and neo-hesperidin, with defined composition and concentration of flavonoids. By observing the mucosal of rats, we found that the small intestinal mucosal injury in the PTFC prevention group was better than that in the NSAIDs group, thus confirming that PTFC may have a preventive effect in a concentration-dependent manner on NSAIDs-induced intestinal lesions. However, the specific prevention mechanism is still unclear.

Exosomes, with diameters ranging from 40 to 160 nm, are secreted from cells via the exocytosis of endosomes. The interior of exosomes is rich in proteins, lipids, DNA, and RNA (miRNA, mRNA, lncRNA), sourced from the cells. Once these exosomes are endocytosed by recipient cells, their contents will be released to enable signaling across cells [47,48]. We speculate that exosomes may be the key to affecting normal IECs and exacerbating NSAIDs enteropathy. Therefore, we extracted exosomes from the above rat small intestine tissue and co-cultured them with IEC-6 cells. We found that the autophagy and intestinal mucosal mechanical barrier function of IEC6 cells were reduced after co-culture with exosomes from rats in the NSAIDs group. By contrast, the autophagy and intestinal mucosal mechanical barrier function of IEC-6 cells co-cultured with PTFC intervention group rat-derived exosomes were better. Autophagy is a degradation mechanism with cytoprotective functions, widespread in eukaryotes. Through the combination of autophagosome and lysosome, cells actively degrade damaged cells and invading bacteria, maintaining the stability of the intracellular environment [49–52]. Studies have found that autophagy is crucial in maintaining the survival of IECs [53] and has a direct regulatory relationship with the intestinal mucosal mechanical barrier function [54]. The dysfunction of the intestinal mucosal mechanical barrier is the core mechanism of intestinal lesions caused by NSAIDs: the dysfunction of the intestinal mucosal mechanical barrier will increase the permeability of the intestinal mucosa, leading to mucosal ulcers, bleeding, perforation, and other lesions [55,56]. The results of the co-culture experiment of IEC-6 cells and exosomes suggested that exosomes did affect the autophagy and intestinal mucosal barrier function of IEC-6 cells, which may be the relevant mechanism for the deterioration of NSAIDs enteropathy. The lncRNA-H19 inside exosomes may be the critical regulatory RNA.

Subsequently, in order to clarify the regulatory relationship between lncRNA-H19 and autophagy/intestinal mechanical barrier and to exclude the potential influence of IEC-6's own lncRNA-H19, we interfered with the lncRNA-H19 expression of IEC-6 cells, then co-cultured with exosomes. The results showed that both in the scramble or shRNA-H19 groups, after co-culture with exosomes from rats in the NSAIDs group, the autophagy level of IEC6 cells was reduced, and the intestinal mucosal mechanical barrier function was

disrupted. The levels of autophagy and mechanical barrier function of IEC-6 cells co-cultured with exosomes extracted from rats in the $PTFC_{high}$ prevention group were still lower than those in the normal control but were significantly better than the NSAIDs group. This result further supports that autophagy and intestinal mucosal barrier function in IEC-6 cells are mainly affected by exosome-derived lncRNA-H19 rather than the lncRNA H19 of IEC-6 cells. Simultaneously, we analyzed the co-culture results of IEC-6 in the scramble and shRNA-H19 groups with exosomes extracted from the same group of rats. The results showed that after inhibiting the expression of lncRNA H19, the autophagy level and intestinal mucosal mechanical barrier function of IEC-6 cells were increased, suggesting that low expression of lncRNA H19 could improve autophagy and intestinal barrier function.

However, there might be some limits in the study due to the poor water solubility of PTFC. Chemical modification of pharmacophores or combining nanoparticle systems should be investigated in further study to help improve the water solubility and bioavailability of the drug. Integrating active components of PTFC with exosomes may also be a promising future research direction for drug development. Future clinical trials will also be needed to validate the effective human dosage of PTFC.

5. Conclusion

Collectively, we successfully showed the regulation of PTFC to exosomal lncRNA H19 expression, and confirmed the regulatory relationship between exosomal lncRNA-H19/autophagy/intestinal mucosal mechanical barrier. PTFC protected intestinal barrier integrity by down-regulating exosomal lncRNA H19 and promoting autophagy, suggesting the potential therapeutic application of PTFC in the treatment of NSAIDs-related intestinal lesions.

Ethics approval and consent to participate

The animal study was approved by the Institutional Animal Care and Use Committee of Zhejiang Chinese Medical University (Approval No. IACUC-20210712-10). All animal care (including the euthanasia procedure) was done with the guidelines of the Association for Assessment and Accreditation of Laboratory Animal Care (AAALAC) and the Institutional Animal Care and Use Committee (IACUC).

Funding statement

The work was supported by Zhejiang Medical and Health Science and Technology Plan Project (2023KY850, 2021KY834), National Natural Science Foundation (82074214), Zhejiang Traditional Chinese Medicine Administration (2023ZL417), Medical Research Development Fund Project of the Beijing Kangmeng Charity Foundation (No. WS686F), and Leading Talents of Scientific and Technological Innovation in the “ten thousand talents plan” of Zhejiang Province (2020R52024).

Data availability statement

The data that support the findings of this study have not been deposited into a publicly available repository, but are available from the corresponding author upon reasonable request.

CRediT authorship contribution statement

Shanshan Chen: Visualization, Validation, Project administration, Methodology, Conceptualization. **Ruonan He:** Writing – review & editing, Writing – original draft. **Ying Li:** Data curation. **Shuo Zhang:** Writing – review & editing, Supervision, Project administration, Funding acquisition, Conceptualization.

Declaration of competing interest

The authors declare that they have no known competing financial interests or personal relationships that could have appeared to influence the work reported in this paper.

Acknowledgements

We thank the Zhejiang Chinese Medical University for its experimental support and research facility.

Abbreviation

NSAIDs	Non-steroid anti-inflammatory drugs
IEC	Intestinal epithelial cell
PTFC	Pure total flavonoids from Citrus
SD	Sprague–Dawley
GI	Gastrointestinal
PPIs	Proton pump inhibitors

FDA U.S. Food and Drug Administration
PI3K Phosphoinositide 3-kinase
AKT Protein kinase B
lncRNA Long noncoding RNA
mTOR Mechanistic target of rapamycin kinase
DIRAS3 DIRAS Family GTPase 3
HSCs Hepatic stellate cells
CRC Colorectal cancer
HCC Hepatocellular carcinoma
i.g. Intragastrical
SPF Specific pathogen-free
AAALAC Association for Assessment and Accreditation of Laboratory Animal Care
IACUC Institutional Animal Care and Use Committee
a.m. Ante meridiem
HPLC High-Performance Liquid Chromatography
DTT Dithiothreitol
PBS Phosphate-buffered saline
EDTA Ethylenediaminetetraacetic acid
WB Western blotting
TEM Transmission electron microscope
BCA Bicinchoninic acid
PVDF Polyvinylidene difluoride
SDS–PAGE Sodium dodecyl sulfate-polyacrylamide gel electrophoresis
ECL Enhanced chemiluminescence
DMEM Dulbecco's Modified Eagle Medium
FBS Fetal bovine serum
SD Standard deviation
qRT-PCR Real-Time Quantitative Reverse Transcription Polymerase Chain Reaction
EVs Extracellular vesicles
rt Room temperature
DAPI 4′6-diamidino-2-phenylindole
ANOVA Analysis of Variance
DSS Dextran sulfate sodium
miRNA MicroRNA
mRNA Messenger RNA
MSCs Mesenchymal stem cells
PE Phosphatidylethanolamine
MAP-LC3 Microtubule Associated Protein 1 Light Chain 3 Alpha
Atg5 Autophagy related 5
AV Autophagic vacuole
PG Prostaglandin
R&D Research and development

Appendix A. Supplementary data

Supplementary data to this article can be found online at https://doi.org/10.1016/j.heliyon.2024.e29797.

References

[1] J.N. Cashman, The mechanisms of action of NSAIDs in analgesia, Drugs 52 (1996) 13–23, https://doi.org/10.2165/00003495-199600525-00004.
[2] G. Gargiulo, D. Capodanno, G. Longo, P. Capranzano, C. Tamburino, Updates on NSAIDs in patients with and without coronary artery disease: pitfalls, interactions and cardiovascular outcomes, Expet Rev. Cardiovasc. Ther. 12 (2014) 1185–1203, https://doi.org/10.1586/14779072.2014.964687.
[3] C.-C. Szeto, K. Sugano, J.-G. Wang, K. Fujimoto, S. Whittle, G.K. Modi, C.-H. Chen, J.-B. Park, L.-S. Tam, K. Vareesangthip, K.K.F. Tsoi, F.K.L. Chan, Non-steroidal anti-inflammatory drug (NSAID) therapy in patients with hypertension, cardiovascular, renal or gastrointestinal comorbidities: joint APAGE/APLAR/APSDE/APSH/APSN/PoA recommendations, Gut 69 (2020) 617–629, https://doi.org/10.1136/gutjnl-2019-319300.
[4] K.K. Boyina, G. Nakkana, V.R.V. Murthy, Buying over-the-counter antacid products containing aspirin? FDA drug safety communication for serious bleeding risk, Am. J. Gastroenterol. 112 (2017) 654–655, https://doi.org/10.1038/ajg.2016.597.
[5] K. Higuchi, E. Umegaki, T. Watanabe, Y. Yoda, E. Morita, M. Murano, S. Tokioka, T. Arakawa, Present status and strategy of NSAIDs-induced small bowel injury, J. Gastroenterol. 44 (2009) 879–888, https://doi.org/10.1007/s00535-009-0102-2.
[6] D.E. Freedberg, L.S. Kim, Y.-X. Yang, The risks and benefits of long-term use of proton pump inhibitors: expert review and best practice advice from the American gastroenterological association, Gastroenterology 152 (2017) 706–715, https://doi.org/10.1053/j.gastro.2017.01.031.

[7] I. Bjarnason, C. Scarpignato, E. Holmgren, M. Olszewski, K.D. Rainsford, A. Lanas, Mechanisms of damage to the gastrointestinal tract from nonsteroidal anti-inflammatory drugs, Gastroenterology 154 (2018) 500–514, https://doi.org/10.1053/j.gastro.2017.10.049.

[8] C. Zihni, C. Mills, K. Matter, M.S. Balda, Tight junctions: from simple barriers to multifunctional molecular gates, Nat. Rev. Mol. Cell Biol. 17 (2016) 564–580, https://doi.org/10.1038/nrm.2016.80.

[9] M. Wong, A.S. Ganapathy, E. Suchanec, L. Laidler, T. Ma, P. Nighot, Intestinal epithelial tight junction barrier regulation by autophagy-related protein ATG6/beclin 1, Am. J. Physiol. Cell Physiol. 316 (2019) C753–C765, https://doi.org/10.1152/ajpcell.00246.2018.

[10] S. Chen, J. Jiang, G. Chao, X. Hong, H. Cao, S. Zhang, Pure total flavonoids from citrus protect against nonsteroidal anti-inflammatory drug-induced small intestine injury by promoting autophagy in vivo and in vitro, Front. Pharmacol. 12 (2021) 622744, https://doi.org/10.3389/fphar.2021.622744.

[11] C. Zhuo, R. Jiang, X. Lin, M. Shao, LncRNA H19 inhibits autophagy by epigenetically silencing of DIRAS3 in diabetic cardiomyopathy, Oncotarget 8 (2017) 1429–1437, https://doi.org/10.18632/oncotarget.13637.

[12] T.-J. Huang, J.-J. Ren, Q.-Q. Zhang, Y.-Y. Kong, H.-Y. Zhang, X.-H. Guo, H.-Q. Fan, L.-X. Liu, IGFBPrP1 accelerates autophagy and activation of hepatic stellate cells via mutual regulation between H19 and PI3K/AKT/mTOR pathway, Biomed. Pharmacother. 116 (2019) 109034, https://doi.org/10.1016/j.biopha.2019.109034.

[13] T.-X. Yu, H.K. Chung, L. Xiao, J.-J. Piao, S. Lan, S.K. Jaladanki, D.J. Turner, J.-P. Raufman, M. Gorospe, J.-Y. Wang, Long noncoding RNA H19 impairs the intestinal barrier by suppressing autophagy and lowering paneth and goblet cell function, Cellular and Molecular Gastroenterology and Hepatology 9 (2020) 611–625, https://doi.org/10.1016/j.jcmgh.2019.12.002.

[14] Z. Sun, S. Yang, Q. Zhou, G. Wang, J. Song, Z. Li, Z. Zhang, J. Xu, K. Xia, Y. Chang, J. Liu, W. Yuan, Emerging role of exosome-derived long non-coding RNAs in tumor microenvironment, Mol. Cancer 17 (2018) 82, https://doi.org/10.1186/s12943-018-0831-z.

[15] A.A. Farooqi, N.N. Desai, M.Z. Qureshi, D.R.N. Librelotto, M.L. Gasparri, A. Bishayee, S.M. Nabavi, V. Curti, M. Daglia, Exosome biogenesis, bioactivities and functions as new delivery systems of natural compounds, Biotechnol. Adv. 36 (2018) 328–334, https://doi.org/10.1016/j.biotechadv.2017.12.010.

[16] K.M. Kim, K. Abdelmohsen, M. Mustapic, D. Kapogiannis, M. Gorospe, RNA in extracellular vesicles, WIREs RNA 8 (2017) e1413, https://doi.org/10.1002/wrna.1413.

[17] X. Li, R. Liu, Z. Huang, E.C. Gurley, X. Wang, J. Wang, H. He, H. Yang, G. Lai, L. Zhang, J.S. Bajaj, M. White, W.M. Pandak, P.B. Hylemon, H. Zhou, Cholangiocyte-derived exosomal long noncoding RNA H19 promotes cholestatic liver injury in mouse and humans, Hepatology 68 (2018) 599–615, https://doi.org/10.1002/hep.29838.

[18] R. Liu, X. Li, W. Zhu, Y. Wang, D. Zhao, X. Wang, E.C. Gurley, G. Liang, W. Chen, G. Lai, W.M. Pandak, H. Robert Lippman, J.S. Bajaj, P.B. Hylemon, H. Zhou, Cholangiocyte-derived exosomal long noncoding RNA H19 promotes hepatic stellate cell activation and cholestatic liver fibrosis, Hepatology 70 (2019) 1317–1335, https://doi.org/10.1002/hep.30662.

[19] A. Conigliaro, V. Costa, A. Lo Dico, L. Saieva, S. Buccheri, F. Dieli, M. Manno, S. Raccosta, C. Mancone, M. Tripodi, G. De Leo, R. Alessandro, CD90+ liver cancer cells modulate endothelial cell phenotype through the release of exosomes containing H19 lncRNA, Mol. Cancer 14 (2015) 155, https://doi.org/10.1186/s12943-015-0426-x.

[20] Y. Chen, H. Ding, M. Wei, W. Zha, S. Guan, N. Liu, Y. Li, Y. Tan, Y. Wang, F. Wu, MSC-secreted exosomal H19 promotes trophoblast cell invasion and migration by downregulating let-7b and upregulating FOXO1, Mol. Ther. Nucleic Acids 19 (2020) 1237–1249, https://doi.org/10.1016/j.omtn.2019.11.031.

[21] J. Ren, L. Ding, D. Zhang, G. Shi, Q. Xu, S. Shen, Y. Wang, T. Wang, Y. Hou, Carcinoma-associated fibroblasts promote the stemness and chemoresistance of colorectal cancer by transferring exosomal lncRNA H19, Theranostics 8 (2018) 3932–3948, https://doi.org/10.7150/thno.25541.

[22] B. He, J. Jiang, Z. Shi, L. Wu, J. Yan, Z. Chen, M. Luo, D. Cui, S. Xu, M. Yan, S. Zhang, Z. Chen, Pure total flavonoids from citrus attenuate non-alcoholic steatohepatitis via regulating the gut microbiota and bile acid metabolism in mice, Biomed. Pharmacother. 135 (2021) 111183, https://doi.org/10.1016/j.biopha.2020.111183.

[23] Y. Hu, J. Liu, H. Li, W. Tang, X. Li, Y. Guo, Chemical constituents from *Citrus changshan-huyou* and their anti-inflammatory activities, Chem. Biodivers. 17 (2020) e2000503, https://doi.org/10.1002/cbdv.202000503.

[24] G. Chao, S. Zhang, Therapeutic effects of muscovite to non-steroidal anti-inflammatory drugs-induced small intestinal disease, Int. J. Pharm. 436 (2012) 154–160, https://doi.org/10.1016/j.ijpharm.2012.05.063.

[25] F. Xia, F. Ding, Y. Lv, W. Di, Y. Sheng, G. Ding, A high efficient method to isolate exosomes from small intestinal epithelium, Mol. Biotechnol. 61 (2019) 325–331, https://doi.org/10.1007/s12033-019-00163-9.

[26] K.J. Livak, T.D. Schmittgen, Analysis of relative gene expression data using real-time quantitative PCR and the $2^{-\Delta\Delta CT}$ method, Methods 25 (2001) 402–408, https://doi.org/10.1006/meth.2001.1262.

[27] A. Quaroni, D. Calnek, E. Quaroni, J.S. Chandler, Keratin expression in rat intestinal crypt and villus cells. Analysis with a panel of monoclonal antibodies, J. Biol. Chem. 266 (1991) 11923–11931.

[28] L. Wang, X. Wang, Z. Shi, L. Shen, J. Zhang, J. Zhang, Bovine milk exosomes attenuate the alteration of purine metabolism and energy status in IEC-6 cells induced by hydrogen peroxide, Food Chem. 350 (2021) 129142, https://doi.org/10.1016/j.foodchem.2021.129142.

[29] D. Gupta, A.M. Zickler, S. El Andaloussi, Dosing extracellular vesicles, Adv. Drug Deliv. Rev. 178 (2021) 113961, https://doi.org/10.1016/j.addr.2021.113961.

[30] M.A. Rivoira, V. Rodriguez, G. Talamoni, N. Tolosa De Talamoni, New perspectives in the pharmacological potential of naringin in medicine, Comput. Mater. Continua (CMC) 28 (2021) 1987–2007, https://doi.org/10.2174/0929867327666200604171351.

[31] H. Cao, J. Liu, P. Shen, J. Cai, Y. Han, K. Zhu, Y. Fu, N. Zhang, Z. Zhang, Y. Cao, Protective effect of naringin on DSS-induced ulcerative colitis in mice, J. Agric. Food Chem. 66 (2018) 13133–13140, https://doi.org/10.1021/acs.jafc.8b03942.

[32] P.I. Oteiza, C.G. Fraga, D.A. Mills, D.H. Taft, Flavonoids and the gastrointestinal tract: local and systemic effects, Mol. Aspect. Med. 61 (2018) 41–49, https://doi.org/10.1016/j.mam.2018.01.001.

[33] R. Cao, X. Wu, H. Guo, X. Pan, R. Huang, G. Wang, J. Liu, Naringin exhibited therapeutic effects against DSS-induced mice ulcerative colitis in intestinal barrier–dependent manner, Molecules 26 (2021) 6604, https://doi.org/10.3390/molecules26216604.

[34] D.I. Hamdan, M.F. Mahmoud, M. Wink, A.M. El-Shazly, Effect of hesperidin and neohesperidin from bittersweet orange (Citrus aurantium var. bigaradia) peel on indomethacin-induced peptic ulcers in rats, Environ. Toxicol. Pharmacol. 37 (2014) 907–915, https://doi.org/10.1016/j.etap.2014.03.006.

[35] S. Mitra, M.S. Lami, T.M. Uddin, R. Das, F. Islam, J. Anjum, MdJ. Hossain, T.B. Emran, Prospective multifunctional roles and pharmacological potential of dietary flavonoid narirutin, Biomed. Pharmacother. 150 (2022) 112932, https://doi.org/10.1016/j.biopha.2022.112932.

[36] C. Li, H. Schluesener, Health-promoting effects of the citrus flavanone hesperidin, Crit. Rev. Food Sci. Nutr. 57 (2017) 613–631, https://doi.org/10.1080/10408398.2014.906382.

[37] S. Tejada, S. Pinya, M. Martorell, X. Capó, J.A. Tur, A. Pons, A. Sureda, Potential anti-inflammatory effects of hesperidin from the genus citrus, Comput. Mater. Continua (CMC) 25 (2019) 4929–4945, https://doi.org/10.2174/0929867324666170718104412.

[38] M. Mathieu, N. Névo, M. Jouve, J.I. Valenzuela, M. Maurin, F.J. Verweij, R. Palmulli, D. Lankar, F. Dingli, D. Loew, E. Rubinstein, G. Boncompain, F. Perez, C. Théry, Specificities of exosome versus small ectosome secretion revealed by live intracellular tracking of CD63 and CD9, Nat. Commun. 12 (2021) 4389, https://doi.org/10.1038/s41467-021-24384-2.

[39] A. Hoshino, H.S. Kim, L. Bojmar, K.E. Gyan, M. Cioffi, J. Hernandez, C.P. Zambirinis, G. Rodrigues, H. Molina, S. Heissel, M.T. Mark, L. Steiner, A. Benito-Martin, S. Lucotti, A. Di Giannatale, K. Offer, M. Nakajima, C. Williams, L. Nogués, F.A. Pelissier Vatter, A. Hashimoto, A.E. Davies, D. Freitas, C.M. Kenific, Y. Ararso, W. Buehring, P. Lauritzen, Y. Ogitani, K. Sugiura, N. Takahashi, M. Alečković, K.A. Bailey, J.S. Jolissant, H. Wang, A. Harris, L.M. Schaeffer, G. García-Santos, Z. Posner, V.P. Balachandran, Y. Khakoo, G.P. Raju, A. Scherz, I. Sagi, R. Scherz-Shouval, Y. Yarden, M. Oren, M. Malladi, M. Petriccione, K.C. De Braganca, M. Donzelli, C. Fischer, S. Vitolano, G.P. Wright, L. Ganshaw, M. Marrano, A. Ahmed, J. DeStefano, E. Danzer, M.H.A. Roehrl, N.J. Lacayo, T. C. Vincent, M.R. Weiser, M.S. Brady, P.A. Meyers, L.H. Wexler, S.R. Ambati, A.J. Chou, E.K. Slotkin, S. Modak, S.S. Roberts, E.M. Basu, D. Diolaiti, B.A. Krantz, F. Cardoso, A.L. Simpson, M. Berger, C.M. Rudin, D.M. Simeone, M. Jain, C.M. Ghajar, S.K. Batra, B.Z. Stanger, J. Bui, K.A. Brown, V.K. Rajasekhar, J.H. Healey, M. De Sousa, K. Kramer, S. Sheth, J. Baisch, V. Pascual, T.E. Heaton, M.P. La Quaglia, D.J. Pisapia, R. Schwartz, H. Zhang, Y. Liu, A. Shukla, L. Blavier, Y. A. DeClerck, M. LaBarge, M.J. Bissell, T.C. Caffrey, P.M. Grandgenett, M.A. Hollingsworth, J. Bromberg, B. Costa-Silva, H. Peinado, Y. Kang, B.A. Garcia, E.

M. O'Reilly, D. Kelsen, T.M. Trippett, D.R. Jones, I.R. Matei, W.R. Jarnagin, D. Lyden, Extracellular vesicle and particle biomarkers define multiple human cancers, Cell 182 (2020) 1044–1061.e18, https://doi.org/10.1016/j.cell.2020.07.009.
[40] F. Li, R.D. Vierstra, Autophagy: a multifaceted intracellular system for bulk and selective recycling, Trends Plant Sci. 17 (2012) 526–537, https://doi.org/10.1016/j.tplants.2012.05.006.
[41] B. Levine, G. Kroemer, Biological functions of autophagy genes: a disease perspective, Cell 176 (2019) 11–42, https://doi.org/10.1016/j.cell.2018.09.048.
[42] T. Ma, J. Li, Y. Xu, C. Yu, T. Xu, H. Wang, K. Liu, N. Cao, B. Nie, S. Zhu, S. Xu, K. Li, W. Wei, Y. Wu, K. Guan, S. Ding, Atg5-independent autophagy regulates mitochondrial clearance and is essential for iPSC reprogramming, Nat. Cell Biol. 17 (2015) 1379–1387, https://doi.org/10.1038/ncb3256.
[43] O. Beutel, R. Maraspini, K. Pombo-García, C. Martin-Lemaitre, A. Honigmann, Phase separation of zonula occludens proteins drives formation of tight junctions, Cell 179 (2019) 923–936.e11, https://doi.org/10.1016/j.cell.2019.10.011.
[44] A. Fasano, Zonulin and its regulation of intestinal barrier function: the biological door to inflammation, autoimmunity, and cancer, Physiol. Rev. 91 (2011) 151–175, https://doi.org/10.1152/physrev.00003.2008.
[45] T. Otani, M. Furuse, Tight junction structure and function revisited, Trends Cell Biol. 30 (2020) 1014, https://doi.org/10.1016/j.tcb.2020.10.001.
[46] A. Lanas, F. Sopeña, Nonsteroidal anti-inflammatory drugs and lower gastrointestinal complications, Gastroenterol. Clin. N. Am. 38 (2009) 333–352, https://doi.org/10.1016/j.gtc.2009.03.007.
[47] R. Kalluri, V.S. LeBleu, The biology, function, and biomedical applications of exosomes, Science 367 (2020) eaau6977, https://doi.org/10.1126/science.aau6977.
[48] T. Fang, H. Lv, G. Lv, T. Li, C. Wang, Q. Han, L. Yu, B. Su, L. Guo, S. Huang, D. Cao, L. Tang, S. Tang, M. Wu, W. Yang, H. Wang, Tumor-derived exosomal miR-1247-3p induces cancer-associated fibroblast activation to foster lung metastasis of liver cancer, Nat. Commun. 9 (2018) 191, https://doi.org/10.1038/s41467-017-02583-0.
[49] T. Lamark, T. Johansen, Mechanisms of selective autophagy, Annu. Rev. Cell Dev. Biol. 37 (2021) 143–169, https://doi.org/10.1146/annurev-cellbio-120219-035530.
[50] I. Dikic, Z. Elazar, Mechanism and medical implications of mammalian autophagy, Nat. Rev. Mol. Cell Biol. 19 (2018) 349–364, https://doi.org/10.1038/s41580-018-0003-4.
[51] F. Randow, R.J. Youle, Self and nonself: how autophagy targets mitochondria and bacteria, Cell Host Microbe 15 (2014) 403–411, https://doi.org/10.1016/j.chom.2014.03.012.
[52] R.J. Youle, D.P. Narendra, Mechanisms of mitophagy, Nat. Rev. Mol. Cell Biol. 12 (2011) 9–14, https://doi.org/10.1038/nrm3028.
[53] J.V. Patankar, C. Becker, Cell death in the gut epithelium and implications for chronic inflammation, Nat. Rev. Gastroenterol. Hepatol. 17 (2020) 543–556, https://doi.org/10.1038/s41575-020-0326-4.
[54] E.G. Foerster, T. Mukherjee, L. Cabral-Fernandes, J.D.B. Rocha, S.E. Girardin, D.J. Philpott, How autophagy controls the intestinal epithelial barrier, Autophagy 18 (2022) 86–103, https://doi.org/10.1080/15548627.2021.1909406.
[55] N. Di Tommaso, A. Gasbarrini, F.R. Ponziani, Intestinal barrier in human health and disease, IJERPH 18 (2021) 12836, https://doi.org/10.3390/ijerph182312836.
[56] J.M. Scheiman, NSAID-induced gastrointestinal injury: a focused update for clinicians, J. Clin. Gastroenterol. 50 (2016) 5–10, https://doi.org/10.1097/MCG.0000000000000432.